Supplementary Information (SI)

A rock tumbler for mechanochemistry: generation of a photoactive cocrystal and a metal-organic framework

Christopher Hartwick,[a] Karah Putnam[a], Alexios K. Plessas,[b] Akalanka B. Ekanayake,[a] Cherolyn K. Henke,[a] Michael A. Sinnwell,[a] Alexei V. Tivanski,[a] and Leonard R. MacGillivray*[b]

[a] Department of Chemistry, University of Iowa, IA 52242, United States
[b] Département de Chimie, Université de Sherbrooke, QC J1K 2R1, Canada
∗ Corresponding author.
E-mail address: leonard.macgillivray@usherbrooke.ca

Contents

Materials and methods

All chemical materials were used without modification. A rock tumbler (model 3 LB) was purchased from Harbor Freight. Glass jars were available commercially (volume - height x radius: 140 mL - 3.8 x 4.0 cm and 266 mL - 5.3 x 4.0 cm). Ball bearings were purchased from Breezliy (diameters: 13 mm, 10 mm, 9.5 mm). The number of ball bearing implemented in the experiments is guided by size and filling of the jar. An ultraviolet light panel (365 nm) was purchased from Waveform lighting. NMR spectra were collected using a Bruker AVANCE 400 spectrometer at 400 MHz. PXRD diffractograms were collected on a Bruker d8 Advance Diffractometer with Bragg-Brentano geometry. BET measurements were performed on a Nova Station D, under N_2 atmosphere, at 77 K. SEM images were collected using a JEOL JSM-1T700HR Scanning Electron Microscope with the cocrystals being deposited onto a carbon tape, coated with gold, and imaged at 5 keV and 18000 magnifications with a working distance of 6 mm between the sample and electron source.

Large scale experiments

(Di-Cl-res)·(bpe) (1): Di-Cl-res (982 mg, 5.49 mmol) and bpe (1.0 g, 5.49 mmol) where mixed together in a glass jar (capacity: 266 mL) with 20 stainless steel ball bearings (diameter: 13 mm). The solids where ground in the tumbler for 24 hours in an isolated environment free of any light irradiation, yielding the cocrystal in 100% yield.

(Di-Cl-res)·(tpcb) (2i): Di-Cl-res (982 mg, 5.49 mmol) and bpe (1.0 g, 5.49 mmol) where mixed together in a glass jar (capacity: 266 mL) with 20 – 45 stainless steel ball bearings (diameter: 13 mm). The solids where ground in the tumbler, under UV irradiation (365 nm) and the progress of the photoreaction was monitored by NMR spectroscopy yielding the photoproduct **(2i)** in 88.5 – 96.6% yield in 60 hours.

(Di-Cl-res)·(tpcb) (2ii): Di-Cl-res (269 mg, 1.5 mmol) and bpe (547 mg, 3.0 mmol) where mixed together in a glass jar (capacity: 266 mL) with 20 stainless steel ball bearings (diameter: 13 mm). The solids where ground in the tumbler for 203 hours under UV irradiation (365 nm) and the progress of the photoreaction was monitored by NMR spectroscopy, as shown in Table S 1, yielding the photoproduct **(2ii)** in 97.6 % yield.

ZIF-67 (3): $Co(NO_3)_2{\cdot}6H_2O$ (82 mg, 0.282 mmol), 2-methyl-imidazole (1.0 g, 12.18 mmol), and KOH (150 mg, 2.67 mmol) were mixed together in a glass jar (capacity: 140 mL) with 25 stainless steel ball bearings (diameter: 13 mm) for 3 hours. Finaly the solid product was washed with methanol (3 x 10 mL) and dried in an oven at 80 ^oC.

Small scale experiments

(Di-Cl-res)·(tpcb) (2iii): Di-Cl-res (35.8 mg, 0.2 mmol) and bpe (72.9 mg, 0.4 mmol) where mixed together in a glass vial (10 mL) with 9 stainless steel ball bearings (6 x 8 mm and 3 x 4 mm). The solids where ground in the tumbler for 244 hours under UV irradiation (365 nm) and the progress of the photoreaction was monitored by NMR spectroscopy, as shown in Table S 2, yielding the photoproduct **(2iii)** (same as **(2ii)**) in 73.5 % yield.

NMR data

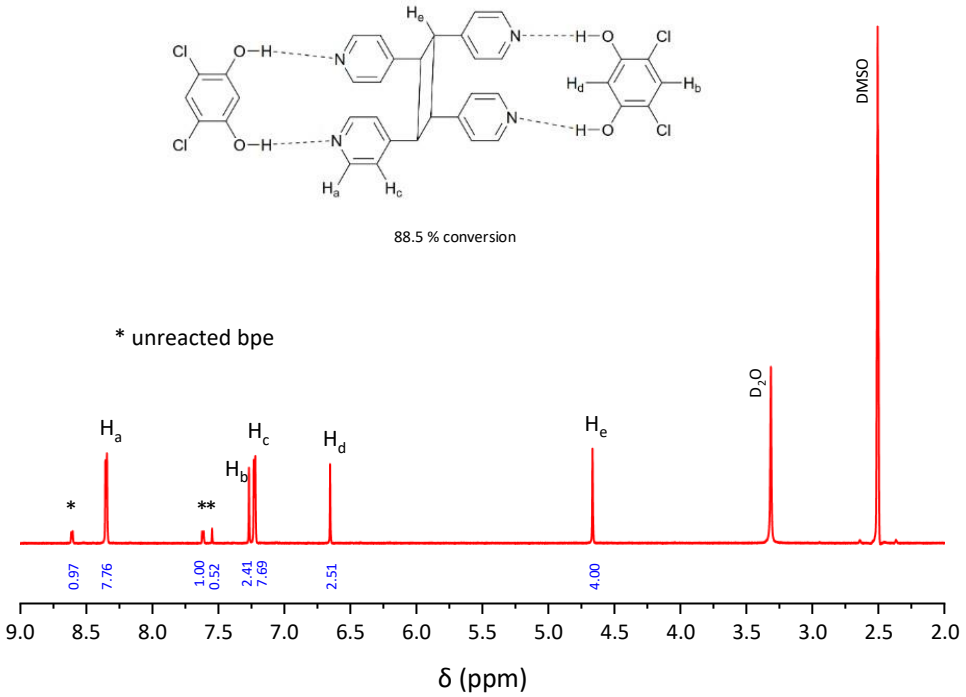

Figure S 1. ^{1}H NMR spectrum of the photoproduct from the 1:1 ratio reaction after grinding with 20 ball bearings for 60 hours. ^{1}H NMR (400 MHz, DMSO-d_6) δ 8.60 (d, 2H), 8.34 (d, 8H), 7.61 (d, 2H), 7.54 (s, 2H), 7.26 (s, 2H), 7.22 (d, 8H), 6.65 (s, 2H), 4.66 (s, 4H).

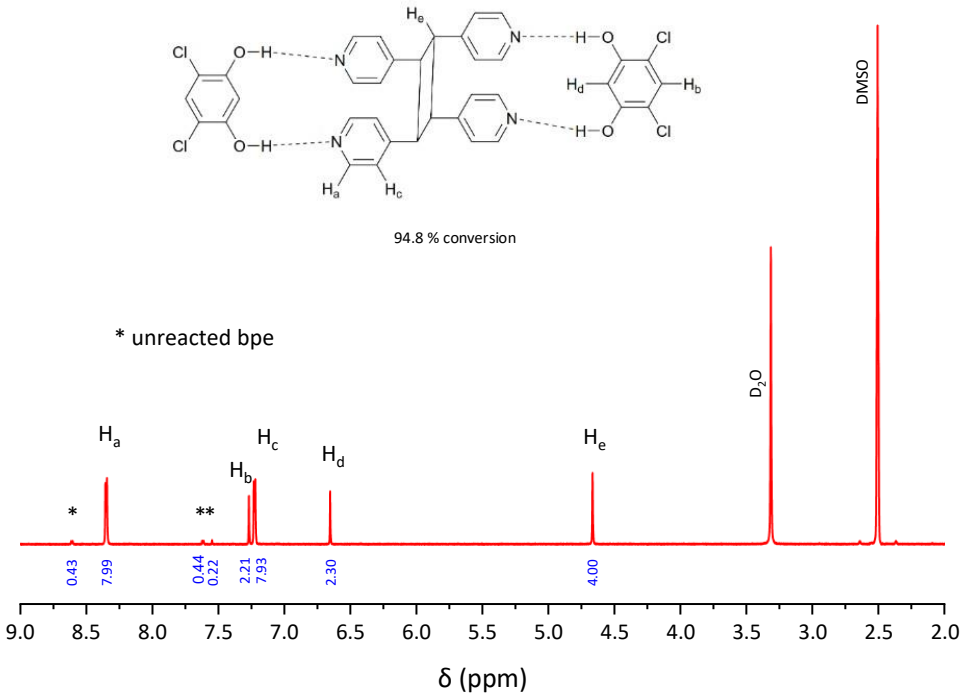

Figure S 2. ^{1}H NMR spectrum of the photoproduct from the 1:1 ratio reaction after grinding with 35 ball bearings for 60 hours. ^{1}H NMR (500 MHz, DMSO-d_6) δ 8.61 (d, J = 5.2 Hz, 0H), 8.35 (d, 8H), 7.62 (d, J = 5.0 Hz, 0H), 7.55 (s, 0H), 7.27 (s, 2H), 7.23 (d, 8H), 6.65 (s, 2H), 4.67 (s, 4H).

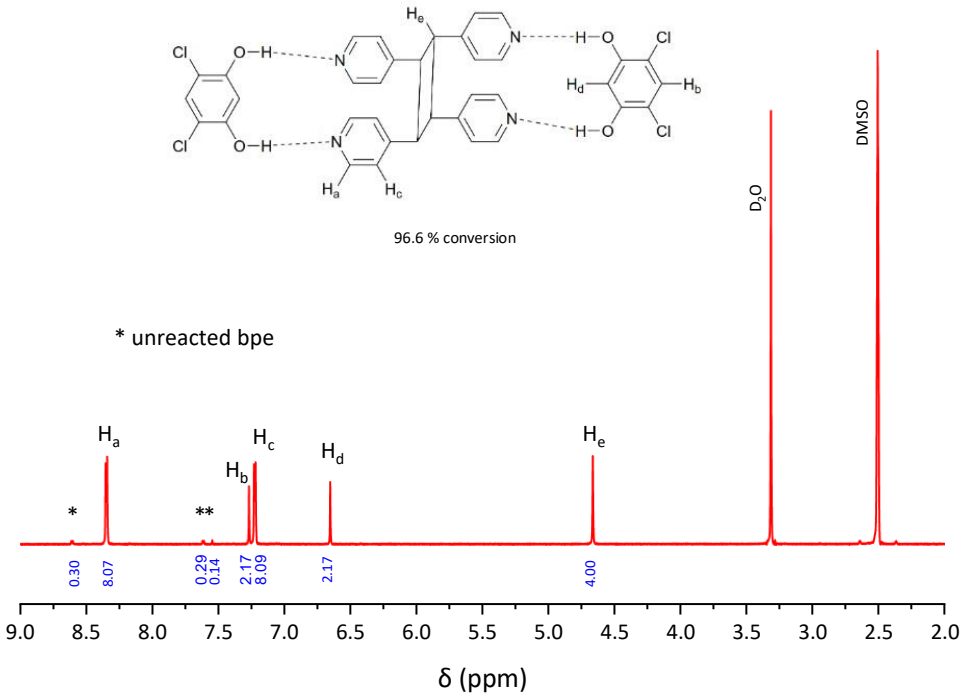

Figure S 3. ^{1}H NMR spectrum of the photoproduct from the 1:1 ratio reaction after grinding with 45 ball bearings for 60 hours. ^{1}H NMR (400 MHz, DMSO-d_6) δ 8.44 (d, J = 5.5 Hz, 2H), 8.18 (d, 1H), 7.45 (d, J = 5.0 Hz, 2H), 7.38 (s, 2H), 7.10 (s, 2H), 7.06 (d, 8H), 6.48 (s, 2H), 4.50 (s, 4H).

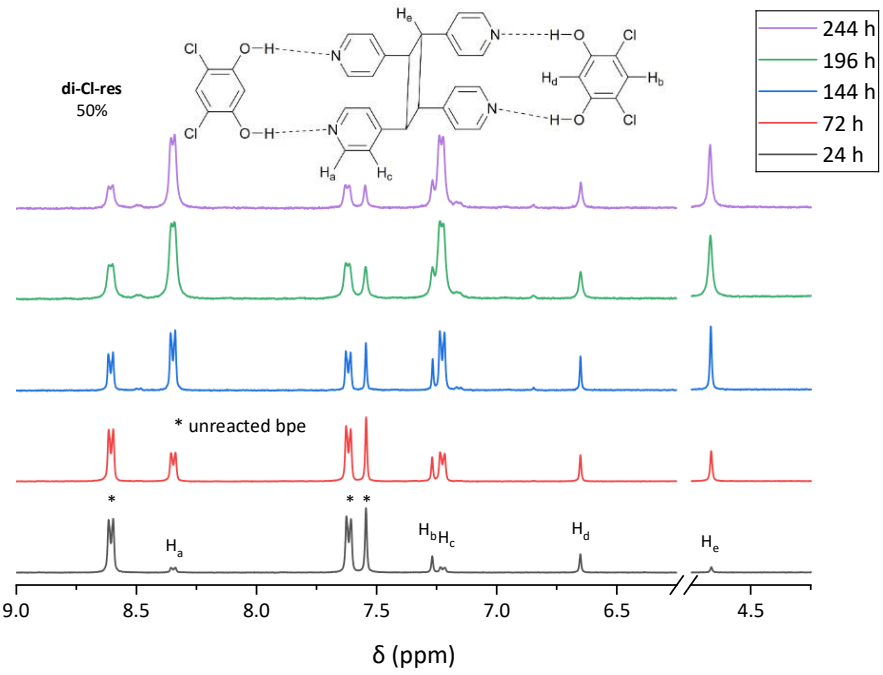

Figure S 4. Stacked ^{1}H NMR spectra of the photoproduct from the catalytic reaction (50% di-Cl-res, small scale) after grinding with 9 ball bearings for various time intervals, zoomed in at the region 9-4 ppm. Horizontal axes break between 6.25 – 4.75 ppm.

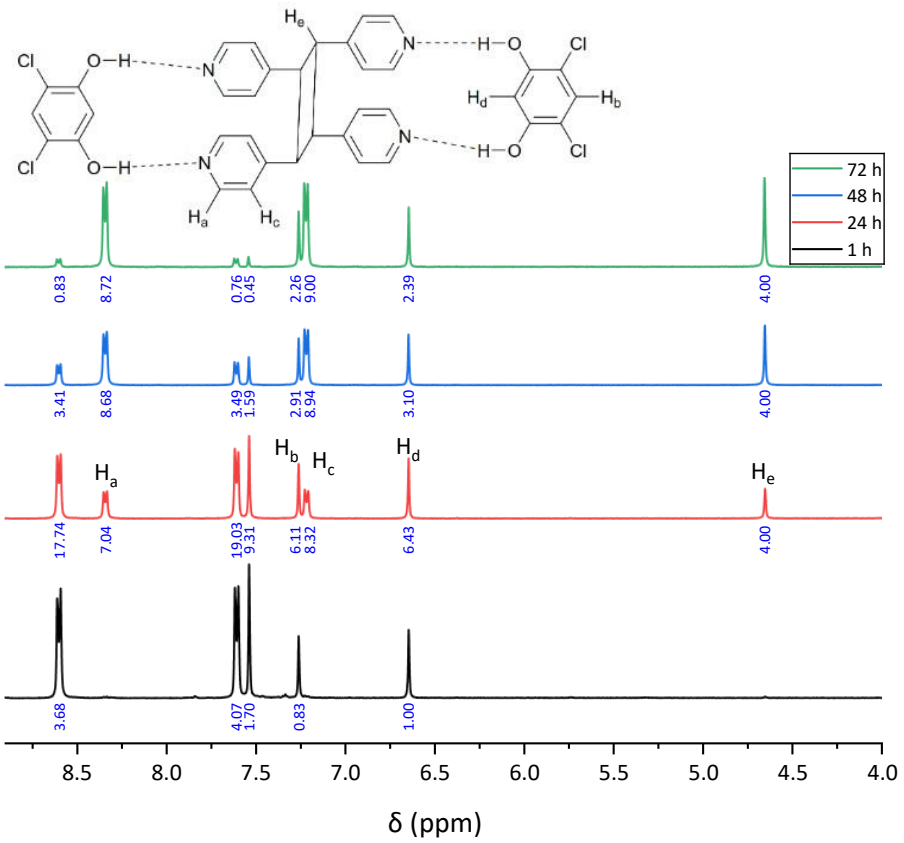

Figure S 5. Stacked NMR spectra of the photoproduct using the presynthesized co-crystal in the tumbler under UV irradiation.

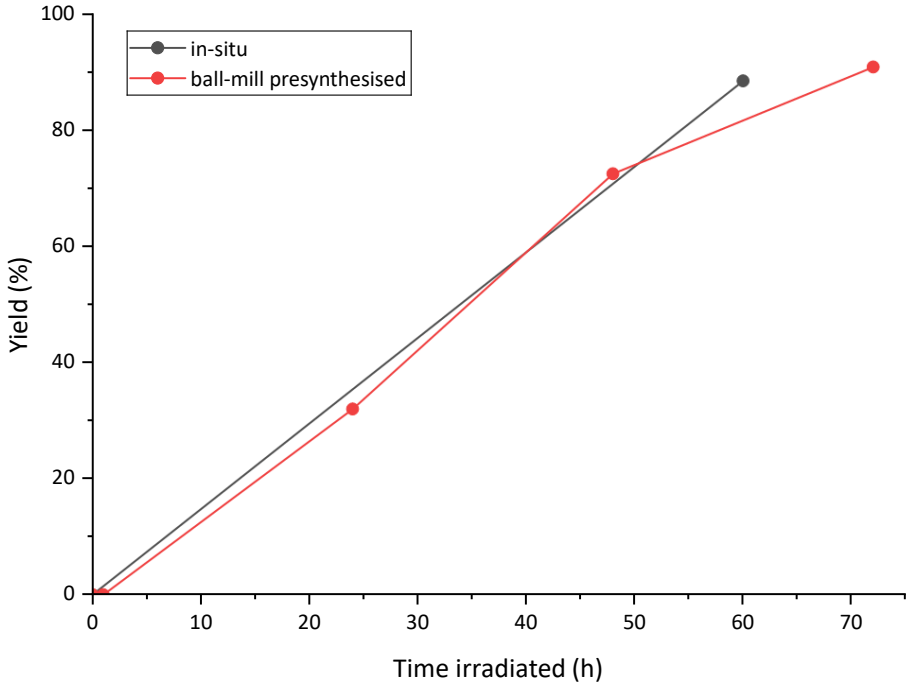

Figure S 6. Graph of yield versus time for photoreaction of the presynthesized co-crystal (red) and the in situ synthesized co-crystal (black).

Catalytic conversion of bpe to tpcb over time in the rock tumbler under UV-radiation

Table S 1. Percentage of bpe converted to tpcb over various time intervals, after grinding with 50% of di-Cl-res, under UV irradiation (large scale experiment).

Time (h)	Conversion
20	1.0 %
40	5.0 %
135	67.0 %
175	84.7 %
203	97.6 %

Table S 2. Percentage of bpe converted to tpcb over various time intervals, after grinding with 50% of di-Cl-res, under UV irradiation (small scale experiment).

Time (h)	Conversion
24	9.9 %
72	37.3 %
144	66.9 %
196	71.2 %
244	73.5 %

Energy calculations illustrating effect of ball bearing loading

In the table below we summarize the results of the calculations made by equations (1) and (2)

$$E_{impact} = \frac{1}{2} m_b v_{eff}^2 \quad (1)$$

$$E_{total} = \varphi E_{impact} N_b f_b t \quad (2)$$

where E_{impact} is derived from the kinetic energy where m_b and u_{eff} are the mass and impact velocity, respectively, of a single ball bearing. For the cumulative energy (E_{total}), φ corresponds to the empirical filling degree of range 0≤ϕ<1, N_b is the total number of balls, f_b is frequency of collisions, and t the total time of grinding.

The calculations are based on literature data on various mechanochemical synthetic routes. The most common used grinding apparatus were shaker mills and planetary mills, while our results are the products of the use of the rock tumbler.

Table S 3. Comparative table of current and commonly used mechanochemical synthetic parameters for reactions.

Reference	Ball bearings		V of container	E_{total} (kJ)	Type of reaction
	number	d (mm)	(mL)		
1	8	10	25	19.1566	1,3-dipolar cycloaddition
2	2	7	10	2.3287	1,3-dipolar cycloaddition
3	6	10	12	15.7642	[4 + 2] cycloaddition reaction
4	4	5	5	3.5398	[3 + 2] cycloaddition reaction
5	3	7	5	12.5128	[3 + 2] cycloaddition reaction
6	6	10	20	1.1725	[3 + 2] cycloaddition reaction
7	1	12	10	20.0683	[4 + 2] cycloaddition reaction
8	1	10.6	10	41.8314	MOF synthesis
9	2	15	10	44.4144	1,3-dipolar cycloaddition
10	1	4.7	25	28.0903	[2 + 1] cycloaddition reaction
11	2	7	5	24.2531	1,3-dipolar cycloaddition
12	1	7	25	4.7736	[4 + 2] cycloaddition reaction
13	1	10	25	93.9296	[4 + 2] cycloaddition reaction
14	1	7	25	3.5802	[4 + 2] cycloaddition reaction
15	1	7	25	3.5802	[4 + 2] cycloaddition reaction
This work	20	13	266	0.0055	[2 + 2] cycloaddition reaction
This work	35	13	266	0.0092	[2 + 2] cycloaddition reaction
This work	45	13	266	0.0112	[2 + 2] cycloaddition reaction
This work	25	13	140	0.0036	MOF synthesis

PXRD data

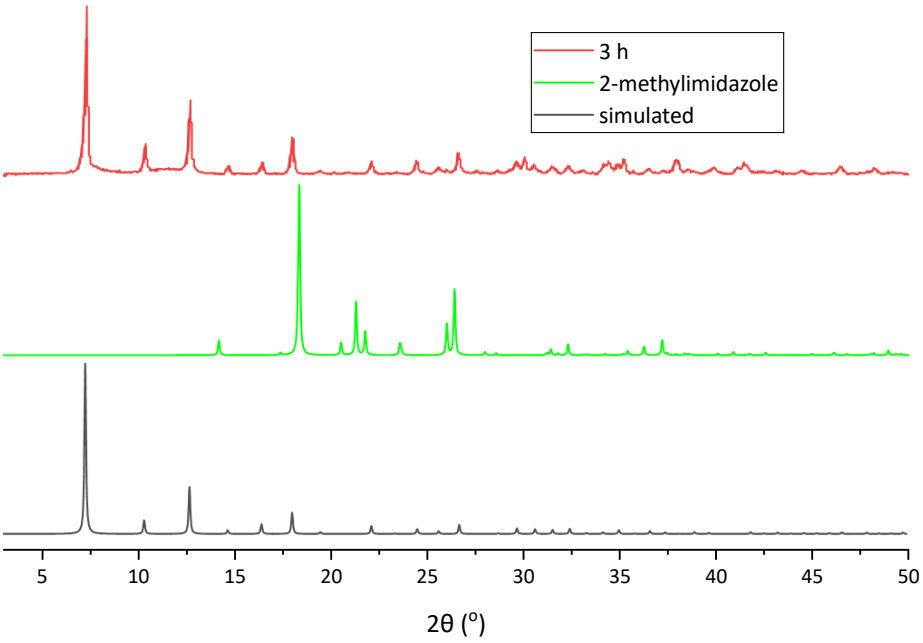

Figure S 7. Stacked PXRD diffractograms of the as synthesized ZIF-67 following wash (red), 2-methylimidazole (green, simulated)[16] and the simulated from the crystal structure (black).[17]

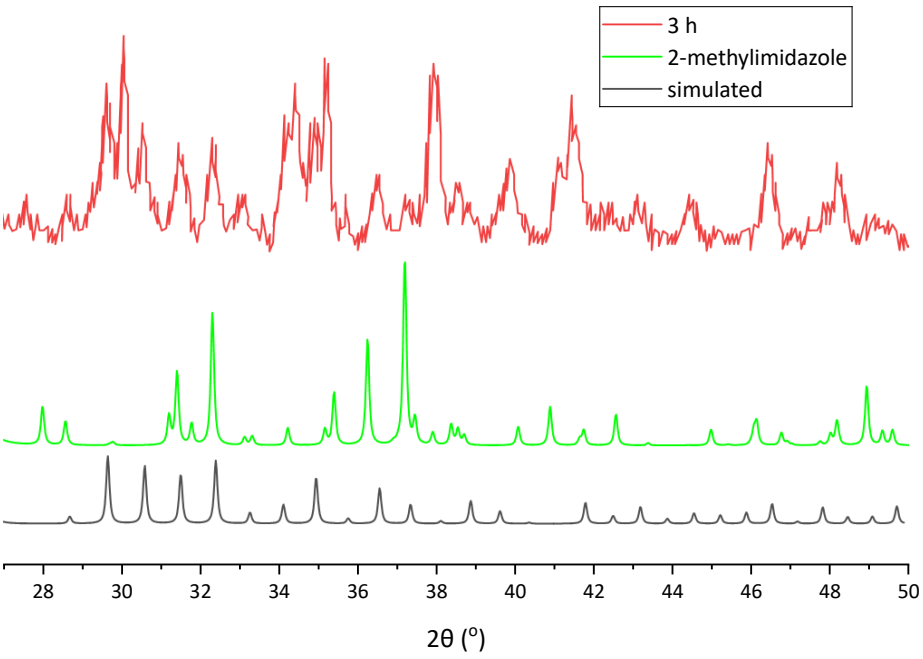

Figure S 8. Stacked PXRD diffractograms of the as synthesized ZIF-67 following wash (red), 2-methylimidazole (green, simulated)[16] and the simulated from the crystal structure (black),[17] zoomed in the range 27° – 50°.

Brunauer–Emmett–Teller (BET) data

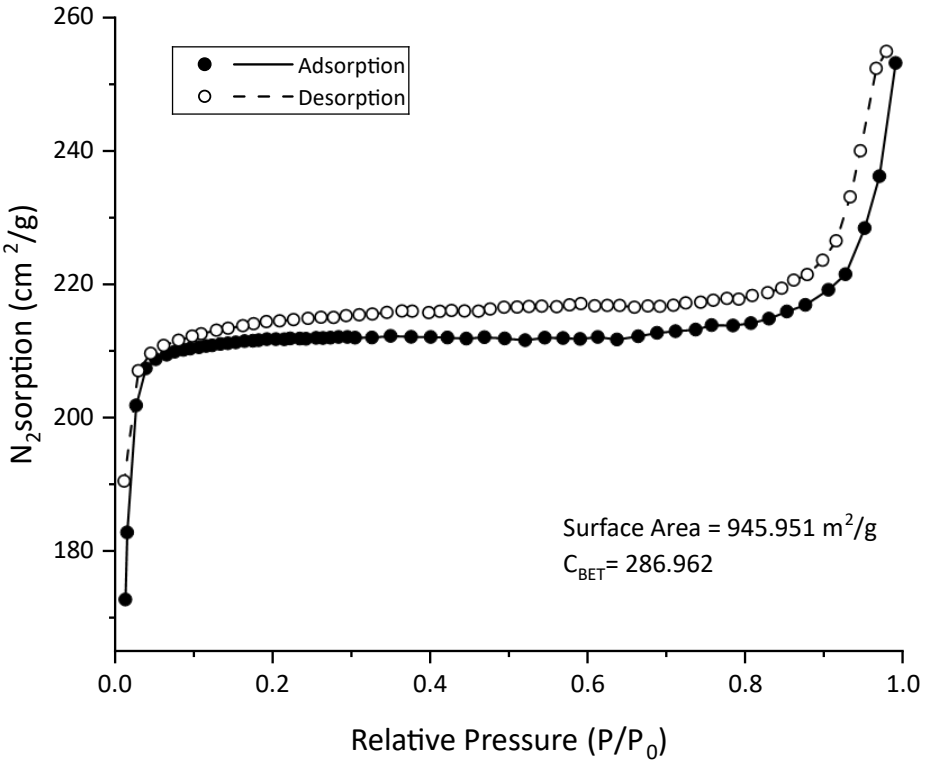

Figure S 9. BET adsorption and desorption graphs of the rock-tumbler-produced ZIF-67, under N_2 atmosphere at 77 K.

Table S 4. Summarizing table of ZIF-67 surface area prepared by various techniques.

Reference	Synthesis		Surface area (m^2 g^{-1})
	M : L : Base ratio	Method	
18	1 : 4 : 4	Aqueous room temperature	608
18	1 : 8 : 8	Aqueous room temperature	636
18	1 : 16 : 16	Aqueous room temperature	868
19	1 : 58 : 0	Aqueous room temperature	1329
19	-	Recycled from above + NaOH	1090
19	-	Recycled from above +Co^{2+}	1322
20	1 : 8 : 0	Methanol, solvothermal	1478
20	1 : 8 : 0	DMF, solvothermal	1168
21	1 : 8 : 0	Methanol, room temperature	2380
22	1 : 58 : 0	Hydrothermal	316
23	1 : 1	Dry grinding (ball mill)	1138
This work	1 : 43 : 9	Dry grinding (tumbler)	945

References

1 R. A. Hernandez R., N. Nabavi, S. J. Patterson and P. Forgione, *ChemCatChem*, 2024, **16**, e202400406.

2 C. Gomes, M. Costa, S. M. M. Lopes, B. A. Nogueira, R. Fausto, J. A. Paixão, T. M. V. D. Pinho e Melo, L. M. D. R. S. Martins and M. Pineiro, *New J. Chem.*, 2023, **48**, 874–886.

3 Y. Wada, K. Tsuchihashi, M. Kanzaki and T. Hamura, *Chem. - A Eur. J.*, 2023, **29**, e202302660.

4 R. K. Fang, Z. C. Yin, J. S. Chen and G. W. Wang, *Green Chem. Lett. Rev.*, 2022, **15**, 519–528.

5 G. Utecht-Jarzyńska, A. Kowalczyk and M. Jasiński, *Molecules*, 2022, **27**, 8446.

6 B. Zhu, W. Li, H. Chen, M. Wu, J. Hu, H. Cao and X. Liu, *Adv. Synth. Catal.*, 2022, **364**, 2911–2915.

7 P. Štrbac and D. Margetić, *Beilstein J. Org. Chem.*, 2022, **18**, 746–753.

8 A. M. Fidelli, A. D. Katsenis, P. Kotidis, G. D. Tarlas, A. Pournara and G. S. Papaefstathiou, *J. Coord. Chem.*, 2022, **74**, 2835–2849.

9 B. Chakraborty, *J. Heterocycl. Chem.*, 2019, **56**, 3414–3422.

10 L. Chen, D. Leslie, M. G. Coleman and J. Mack, *Chem. Sci.*, 2018, **9**, 4650–4661.

11 Z. T. Bhutia, A. Das, M. Biswas, A. Chatterjee and M. Banerjee, *European J. Org. Chem.*, 2018, **2018**, 506–514.

12 Y. J. Tan, F. J. Wang, A. M. Asirib, H. M. Marwanib and Z. Zhang, *J. Chinese Chem. Soc.*, 2018, **65**, 65–73.

13 Y. Zhao, S. V. Rocha and T. M. Swager, *J. Am. Chem. Soc.*, 2016, **138**, 13834–13837.

14 Y. J. Tan, Z. Zhang, F. J. Wang, H. H. Wu and Q. H. Li, *RSC Adv.*, 2014, **4**, 35635–35638.

15 Z. Zhang, Z. W. Peng, M. F. Hao and J. G. Gao, *Synlett*, 2010, 2895–2898.

16 B. Hachuła, M. Nowak and J. Kusz, *J. Chem. Crystallogr.*, 2010, **40**, 201–206.

17 R. Banerjee, A. Phan, B. Wang, C. Knobler, H. Furukawa, M. O'Keeffe and O. M. Yaghi, *Science (80-.).*, 2008, **319**, 939–943.

18 A. F. Gross, E. Sherman and J. J. Vajo, *J. Chem. Soc. Dalt. Trans.*, 2012, **41**, 5458–5460.

19 F. Şahin, B. Topuz and H. Kalıpçılar, *Microporous Mesoporous Mater.*, 2018, **261**, 259–267.

20 J. Ethiraj, S. Palla and H. Reinsch, *Microporous Mesoporous Mater.*, 2020, **294**, 109867.

21 H. Li, H. Ma, X. Wang, J. Gao, C. Chen, S. Shi, M. Qu, N. Feng and J. Xu, *J. Energy Chem.*, 2014, **23**, 742–746.

22 J. Qian, F. Sun and L. Qin, *Mater. Lett.*, 2012, **82**, 220–223.

23 M. Afkhami-Ardekani, M. R. Naimi-Jamal, S. Doaee and S. Rostamnia, *Catalysts*, 2023, **13**, 9.